Journal of Materials Processing Tech. 275 (2020) 116365

Contents lists available at ScienceDirect

Journal of Materials Processing Tech.

journal homepage: www.elsevier.com/locate/jmatprotec

Surface design and texturing of strip steel using nanosecond pulsed lasers for simulated roughness transfer and paint appearance

E. Rodriguez-Vidal[a,*], D.T.A. Matthews[c], V. Sáenz de Viteri[a], F. Korver[b], D.J. Wentink[b], I. Quintana[a]

[a] IK4-TEKNIKER, Polo Tecnológico de Eibar, Calle Iñaki Goenaga, 5, 20600 Eibar, Gipuzkoa, Spain
[b] Tata Steel Research and Development, PO Box 10000, 1970CA, IJmuiden, The Netherlands
[c] Laboratory for Surface Technology and Tribology, Faculty of Engineering Technology, University of Twente, Drienerlolaan 5, 7522 NB Enschede, The Netherlands

ARTICLE INFO

Associate Editor: Prof A Clare

Keywords:
Laser texturing
Nanosecond pulses
Roughness transfer
Surface topography
Paint appearance

ABSTRACT

The final surface topography of flat sheet (galvanized) products is achieved using textured rolls during the skin-pass process. The topography is generally applied to improve the surface functionality of the sheets obtained, or reduce downstream environmental effects. This work analyzes the short-pulse laser texturing technique as an technology to improve a key functionality of galvanized metal sheets for the automotive sector: the paint appearance. For this purpose, deterministic patterns were selected from theoretical methods and produced on imprinting dies by nanosecond pulsed laser processing. The pulsed laser texturing technique has been shown to be highly controllable with suitable reproducibility and surface characteristics in terms of roughness (R_a), peak count (R_{pc}) and waviness (W_a) values, as main factors connected to the desired paint appearance functionality. The roughness transfer capability during the skin-pass process was assessed by normal loading compression tests for different contact pressures and sheet materials. Additionally, the painting process applied in the production chain of automotive parts were reproduced at lab scale, following by the waviness and roughness characterization and validation of the topographic designs proposed. Experimental results show a strong dependence of transfer capability of textures as function of mechanical properties of the metal sheets. For the considered deterministic patterns meaningful differences in terms of transfer capability of R_a and R_{pc} to steel strip were found as function of the pattern topography reaching maximum transfer capability of 60% and 130% for R_a and R_{pc} respectively, for contact pressure range between 250 MPa and 500 MPa, corresponding to maximum absolute values of $R_a = 1.5\,\mu m$ and $R_{pc} = 190\,cm^{-1}$ on the steel strip. Concerning waviness, results revealed a significant decrease of waviness overall length scale considering $R_{pc} > 75 cm^{-1}$ and $0.7\,\mu m < R_a < 1.5\,\mu m$, which involves an enlargement of the current process window with respect to current Electro Discharge Texturing process.

1. Introduction

Surface functionalisation is an increasingly important aspect of modern manufacturing, offering not only more efficient and environmentally friendly solutions to a wide range of applications, but also permitting the exploitation of novel materials and/or coatings. Demir et al., 2013 reported a study of surface topography modification at micro-scale to improve or add new functionalities related to an improvement of adhesion between two dissimilar material or a wear resistance improvement. Costil et al., 2014 analyzed the effect of laser textured dimples on aluminum substrates to promote coating adhesion showing an enhancement of the adhesion strength of up to 300% for the best parameters compared to conventional methods. Surface topography at micro- and nano-scale to improve or add new functionalities such as anti-fouling, and wettability have reached great importance over the past few years. In this sense, Jaggessar et al., 2017 reviewed different fabrication technologies for bio-mimicking structures and theirs effects on wettability properties which are directly related to anti-fouling and bactericide functionalities. Design and manufacturing of the suitable surface topography at microscale level that ensure the predicted surface functionalities remains a key issue to guarantee full exploitation of those surfaces. In particular, optimization of advanced micro-manufacturing technologies is required to face the challenges of current and potential new application areas. These technologies should provide excellent productivity and cost efficiency with good surface finish and integrity. The application area considered in

* Corresponding author.
E-mail address: eva.rodriguez@tekniker.es (E. Rodriguez-Vidal).

https://doi.org/10.1016/j.jmatprotec.2019.116365
Received 21 November 2018; Received in revised form 24 June 2019; Accepted 13 August 2019
Available online 16 August 2019
0924-0136/

this study is the surface modification of rolls to improve the surface functionality of metal sheets obtained during the skin-pass rolling (or temper rolling) process. Skin-pass rolling is usually the final step in the production of cold-rolled steel sheets and is characterized by a small thickness reduction of the sheets (at around 1%). Moreover, the skin-pass rolling is also characterized by the significant role of roughness produced on the roll surface to achieve a certain strip roughness considering the transfer roughness capability which is related to the material being rolled, their elongation during skin-pass rolling and the topography design of the rolling surface. Surface roughness after skin-pass rolling is one of the most important aspects linked to the final product appearance, which means that the roughness transfer capability is a key issue to control during the skin-pass rolling. Thus, the microstructured rollers are commonly used for the manufacturing and processing of flat-rolled steels in the automobile industry to provide a matte finish and improve paint adhesion. The target functionality of this study will be focused on the visual appearance of the painted steel sheet surfaces, which is quantified through the balance among roughness (R_a), peak count (R_{pc}) and waviness (W_a) values as has been previously reported in several studies relating the influence of the steel sheet surface to their appearance after painting. Bastawros et al., 1993 described a comprehensive analysis of the influence of substrates and surface topography on the final paint appearance, finding waviness and peak count as key parameters that can be transmitted through the paint layers. The correlation between roughness parameters and paint appearance was also studied by Scheers et al., 1996Scheers et al., 1998 et al. for patterning carried out by Shot Blasting Texturing (SB) and Electro-Discharge Texturing (EDT) (Stochastic textures) and Sibetex (deterministic). One of their outcomes revealed the fabrication of the the best paint quality (lowest waviness) for deterministic textures. The relevance of these parameters has been summarized in the recently published standard SEP 1941 [SEP, 1941].

Traditionally, surface texturing of mill rolls has been carried out by Shot Blasting Texturing (SB) (De Mello et al., 2013), where stochastic surface roughness is generated by the impact of small steel balls on the roll. This technique has been partially supersede during last decades by Electro Discharge Texturing (EDT), which is based on based on discharge of energy between the two electrodes (electrode and tool electrode) to generate stochastics textures (Elkoca et al., 2008). More recently, Kijima (2014) studied theoretically and experimentally the influence of the radius of EDT textured rolls on roughness transfer capability during skin-pass rolling. The study concluded that the peak pressure between roll and strip surfaces was the most important parameter affecting the roughness transfer capability when large roll radius ($\approx$250 mm) were considered. Roughness transfer simulated by direct normal loading was in good agreement with the rolling experiments performed. Another important factor that affects the roughness transfer capability of EDT textured rolls was the lubrication condition mainly for large roll diameter (Kijima, 2015a; Kijima, 2015b). These studies reported the influence of lubrication of strip elongation and roughness transfer depending on the roll diameter and the profits of considering roll texturing (by EDT) mainly focused on the lubricant retention and the decreasing of the friction coefficient between roll and strip surfaces. The analysis was carried out for two different materials; however the work does not report the influence of different roll roughness values on roughness transfer capability.

Electron Beam Texturing (EBT) (Vermeulen et al., 2001) arose as an alternative to accomplish deterministic surface roughness on mill rolls. However, the EBT technology entails relatively high costs and the need for processing under vacuum. For these reasons, despite the widely acknowledged superior performance in terms of paint and press forming behaviour, the technology has not been adopted in a wide scale by steel-makers. More recently, Laser Surface Texturing (LST) has emerged as a promising technology to guarantee a range of surface designs depending on the desired final function. For example, deterministic and controlled roll surface roughness can be produced to achieve high quality steel sheets. LST is probably the most advanced technique developed for surface texturing of mechanical components due to its promising peculiarities (fast processing time, clean to the environment, no need of vacuum, control of the shape and size of the ablated micro-textures by tuning the characteristic of the laser spot). During LST process, a sequence of laser pulses hit on the workpiece as function of pulse length and repetition rate (frequency). Depending of these laser parameters, high levels of energy density can be deposited on the surface. Laser beam shaping techniques allow to focus the laser beam on a spot with dimensions ranging from few microns to hundreds of microns, which allow to tune the high energy density (fluence) in the spot area. Additionally, the selection of high values of scanning speed makes this technology ideal for industrial upscaling of surface microstructuring compared to conventional machining processes such as EBT. The energy absorbed during the LST process from the laser pulses (in the range of μs to ns) heat the workpiece at temperatures at which the atoms gain enough energy to pass from a liquid to a gaseous state. The mechanisms involve in this transition will mainly depend on the pulse length and the material to be processed, in which the ablation of the material happens through melt expulsion driven by vapour pressure and the recoil pressure of light. After the end of the pulse, the heat is quickly dissipated into the bulk of the material and a recast zone is formed. Thus, it is imperative to find a suitable balance between productivity and the resulting surface finish when selecting the most appropriate ablation regime for laser texturing process Chichkov et al., 1996

Du et al. (2005) investigated the employment of Nd:YAG laser for surface structuring of rolls by theoretical and experimental studies to generate a top-hat shaped bumps on the roll surface. They achieve interesting outcomes related to the increase of surface hardness on the bumps than the matrix which play a crucial role on friction during the forming process of steel sheets. Wan et al. (2008) reported a theoretical research about the application of CO_2 laser radiation by means of a novel laser beam modulating device to texture a cold roller. They evidenced the significant role of energy distribution of the modulated beam on the surface roughness profile after texturing. Additionally, the effect of localised dispersing of hard ceramic particles by pulsed laser radiation on surface integrity was analysed by Hilgenberg et al. (2015), leading to a hardness improvement on pilot rolls used during cold-working steel processes. This technique is focused on increasing surface hardness of rolls, however it makes it difficult to control the roughness parameters to guarantee a certain functionality on the steel strip.

However, only a previous study from the authors examined the roughness transfer capability of micropatterns produced by pulsed laser radiation for improving appearance after painting of steel strip (I. Quintana et al., 2014) although the paint appearance parameters were not the focus of that research.

The main purpose of the present paper is to analyse the laser texturing process as an innovative technology to improve the paint appearance of metal sheets obtained during skin-pass rolling. The LST using ns-pulses was carried out on imprinting dies that are subjected to normal loading compression tests to study the roughness transfer capability for three different substrates during skin-pass rolling. Selective deterministic patterns, established by theoretical methods (Wentink et al., 2015), are considered to study the effect of the topography design, roll material properties and the imprinting parameters (contact pressure) on roughness transfer capability. Furthermore, the waviness of the sheets after imprinting and painting processes was also assessed.

2. Materials and methods

The tool steel material employed in this work as roll surface was a commercially available medium-alloyed cold work tool steel called Uddeholm Rigor® [ref: https://www.uddeholm.com/en/products/uddeholm-rigor/]. This steel is a chemistry and hardness close to typical work roll materials used in steel cold rolling, offering an excellent

Table 1
Bulk and surface roughness parameters of the imprinting sticks.

Material	Hardness [HRc]	Yield Strength [MPa]	R_a [μm]	R_z [μm]	R_t[μm]	R_{pc}[cm^{-1}]
Uddeholm Rigor®	63	190×10^3	0.017	0.14	0.21	≈0

combination of wear and chipping resistance as well as hardenability, being well suited for modern heat treatment processing. Flat samples of $100 \times 30mm^2$ were considered as imprinting dies. Surface roughness parameters (Table 1) were measured by means of a profilometer (Perthometer M2; Mahr GmbH, Göttingen, Germany) considering a cut off wavelength of 2.5 mm [UNE-EN 10049:2013]. R_a is defined as the arithmetic average of the roughness profile; R_{pc} is the number of local roughness peak which project through a selectable band centered about the main line. This parameter is assessed over the evaluation length and is reported in peak per cm. R_{pc} has an important role in this research and it corresponds with the number of local peaks that successively exceed one 0.5 μm upper section line a lower 0.5 μm line (EN, 10049). Peak count (R_{pc}) represents the maximum height of the profile, providing information about the presence or protruding peaks.

Low strength high-formability galvanized steel sheets [TATA Steel] were considered for the imprinting trials: interstitial free low strength high-formability galvanized steel sheet (IF-DX56), rephosphorated-IF (rephos-IF) (YD220) and a dual phase steel (DP600). Different metal sheet dimensions (66×66, 66×50, 66×40, 66×30, $66 \times 20mm^2$) were considered to analyse the effect of contact pressure and material properties on the roughness transfer capability. Subsequently, IF-DX56 material was selected to analyse the paint appearance properties after compression tests.

Table 2 summarizes the surface roughness parameters (cut off length of 2.5 mm) and mechanical properties of the considered metal sheets. Tensile testing was conducted using an INStron Static Universal Machine with a loading rate of 30 MPa/s. Tensile tests were carried out considering applied load parallel to the steel processing (rolling) direction and roughness measurements were made perpendicular to the rolling direction.

A 40 W nanosecond pulsed fiber laser system was used for surface modification of the imprinting dies. The laser delivers pulses in the range 9–250 ns at 1064 nm wavelength, with maximum pulsed energy of 1.3 mJ. The laser beam was guided by a 2D scanner and the assembly was integrated into a micromachining workstation. The sample position can be selected with lateral and depth resolution in the micrometer range through a machining table with X/Y axes and Z positioning system.

The material response to the laser beam interactions and the dimensional characterization of the corresponding transferred patterns on steel sheets were assessed by different methods. Microstructural analysis of the laser ablated substrate was carried out by using a Zeiss Ultra 55 FEG-SEM Ultra Plus at a 15 kV accelerating voltage, followed by ESD analysis of selected areas. Nanoindentation testing to measure changes on hardness on the treatment areas was carried out by a Berkovich tip by a Hysitron triboindenter. Non-contact topographic measurements were conducted using confocal microscopy (Sensofar S- Neox) and Scanning Electron Microscopy (OXFORD INCA Synergy (FE-SEM)).

Compression tests were conducted in a TUWI compression rig with a load capability of 100 tonnes (Fig. 1b). During the experiments, the contact pressure was tuneable by varying the sample size for the values cited above. All tests were performed without lubrication. To guarantee a homogeneous distribution of stress along the textures tool and sheet, FEM simulations of Van Mises stresses were previously conducted using the commercially available MSC Marc software package (Wentink et al., 2015).

Following the imprinting process, painting trials were carried out on a Gorkotte modular pilot paint line comprising the following operations: degreasing, activation, phosphating, passivation and deposition of paint via electrocoating. The paint layers were dried in a Votsch drying chamber.

As commonly applied in the inspection of paint systems, a 55 μm layer of Nitto-Denko 318 Tape (Nitto tape) has been applied to the e-coated surface to negate excessive surface dullness and to simulate the clear topcoat. This simulated paint layer enables the paint appearance to evaluated by measuring the optical waviness of the surfaces by using a Wave-Scan Dual equipment from BYK-Gardner, based on data recorded over 10 mm track length. It simulates visual perception by scanning the wavy light/dark pattern like human eyes. The measurement signal is divided into several ranges using mathematical filter functions which provides the form of structure spectrum ranging from 0.3 to 1.2 mm (Short Wavelength SW) and 1.2–12 mm (Long Wavelength LW)

3. Definition of the laser texture patterns

Paint appearance is related to the roughness (R_a), waviness (W_a) and peak count (R_{pc}) (Scheers et al., 1998, Mezghani et al., 2011) of a surface. According to Kimura et al. (2009), improvements on paint appearance (based on SEP, 1941 Measurement of the waviness characteristic value Wsa(1–5) on cold rolled metallic flat products (2012)) are reached when these parameters reach the following values: $R_{pc} > 75\ cm^{-1}$, $0.7\ \mu m < R_a < 1.5\ \mu m$ and $0.1\ \mu m < W_a < 0.4\ \mu m$. In order to determine, by 3D geometric models, a set of surface texture patterns whose surface parameters fit well with the values cited above, the material response to the pulsed laser radiation has to be evaluated. The texture patterns considered include a non-overlapping matrix of micro-dimples ($\varphi \approx 65\ \mu m$ inner diameter, peak-to-valley depth $D \approx 13\ \mu m$ and recast material width $l \approx 12\ \mu m$) produced on the Uddeholm Rigor polished imprinting dye (Quintana et al. (2014)). The process parameters selected for the production of those single craters were pulse length $\tau = 170$ ns, frequency rate $f = 41$ kHz, speed $v = 3.28$ m/s, average power $P = 19$ W and a four-time repetition of laser shots over the same area to reach the crater depth determined by geometrical design. Fig. 2 shows the confocal image of an isolated crater of a trench of craters on the microstructuring imprinting die. The roughness parameters for the roll textured surface (negative) were $R_a = 5.5\ \mu m$ and $R_{pc} = 100\ cm^{-1}$, significant higher roughness values than target values on strip material. It enables to consider a wide range of contact pressures and roughness transfer percentages during imprinting tests to reach the target roughness properties on strip materials. Fig. 3 a) and b) show the cross section of ablated craters obtained via optical

Table 2
Bulk and surface roughness parameters of galvanized steel sheets used during the imprinting process.

Steel grade	Tensile Strength [MPa]	Yield Strength [MPa]	R_a [μm]	R_{pc}[cm^{-1}]	Wa (0.8-2.5 μm) [μm]
IF-DX56	292 ± 7	122 ± 3	0.5 ± 0.02	20 ± 1.02	0.25 ± 0.02
YD220	386 ± 5	198 ± 7	0.53 ± 0.02	19 ± 1.01	0.27 ± 0.02
DP600	661 ± 12	338 ± 13	0.55 ± 0.01	38 ± 2.2	0.2 ± 0.02

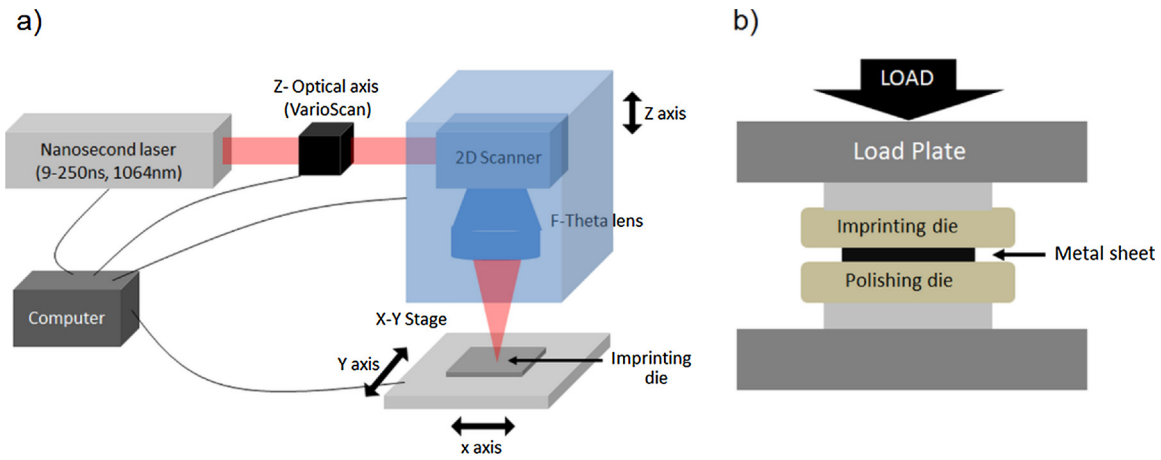

Fig. 1. Schematic view of a) laser experimental setup; b) imprinting tests.

microscopy and SEM respectively. When using nanosecond pulses, the pulse energy is dissipated into the sample in much longer time intervals than the characteristic electro cooling and lattice heating times, which also results in the thermal wave propagation and, as it is shown in Fig. 2a significant ejection of molten material from the bulk followed by its partial re – deposition aside the ablated dimple. The heat affected zone (HAZ) and recast layers are identified in Fig. 3 a), where the microstructure has been modified by the thermal shock produced during the ablation process. In those regions, the material was heated up to temperatures above the melting point and rapidly cooled down, producing a quenching-like process. Nanohardness measurements carried out in the recast layer (8 ± 1 GPa) show lower values as compared with the bulk (11 ± 1 GPa). This is probably caused by the extremely fast cooling rates that take place in those regions, which prevent martensitic transformation and the formation of primary carbides during cooling, producing a softer layer with substantial amounts of retained austenite.

Fig. 4 shows the X-Ray spectral image analysis corresponding to the material composition in the crater after laser ablation. Dotted line (a) indicates the gap or detachment of the epoxy layer (sample preparation for cross section analysis) from the surface. Elements from the steel are polished into the gap. Arrows ((d) and (e)) indicate the slight enrichment of Cr and Mo elements at the HAZ after laser ablation. In general, very low enrichment of elements at the HAZ was observed, which it is connected to the carbide diffusion into that area due to the laser ablation process.

Roughness transfer capability was analyzed by considering the three galvanized steel sheets described in Table 2. A contact pressure range between 0 and 770 MPa was considering during the imprinting trials.

Figs. 5 a) and b) show the surface roughness parameters of the metal sheets obtained after the imprinting process as a function of the nominal contact pressure. Roughness transfer capability (%) is assessed as the ratio between roughness value obtained on the sheet after imprinting tests and the roughness of imprinting die (tool steel). For the three metal sheets considered, an exponential growth was observed for the roughness transfer capability relative to the nominal contact pressure (Fig. 5a). IF-DX56 and YD220 exhibit slightly different behaviour than in the case of DP600 for contact pressure higher than 300 MPa. This result is connected to the different mechanical behaviour for the materials once the yield strength is exceeded (Table 2): for contact pressure values higher than 300–400 MPa, larger roughness transfer capability values are obtained for materials characterized by a lower yield strength. Roughness transfer capability is lower than 60% for R_a for the three substrate materials.

For R_{pc}, we consider the absolute peak countvalues as a function of the nominal contact pressure (Fig. 5 b). This parameter shows a markedly different trend, disclosing a maximum value that depends on the nature (mechanical properties and native R_{pc} values) of the material substrate considered. In the case of DP600 the maximum peak count transfer is reached at around 600 MPa, while in the case of IF-DX56 and YD200 it is reached at 300 MPa and 400 MPa respectively. A peak count transfer drop is observed to contact pressure values higher than the

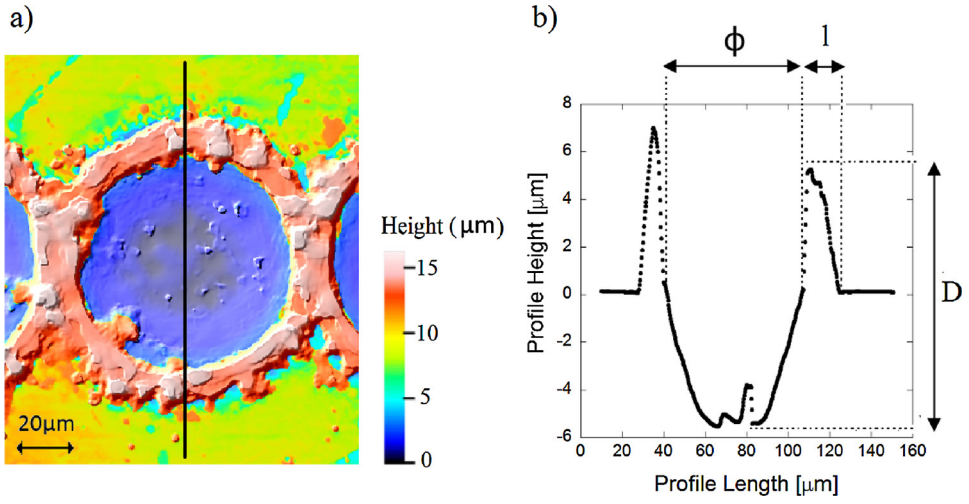

Fig. 2. a) 2D Confocal image; b)cross section profile of the experimental seed pattern.

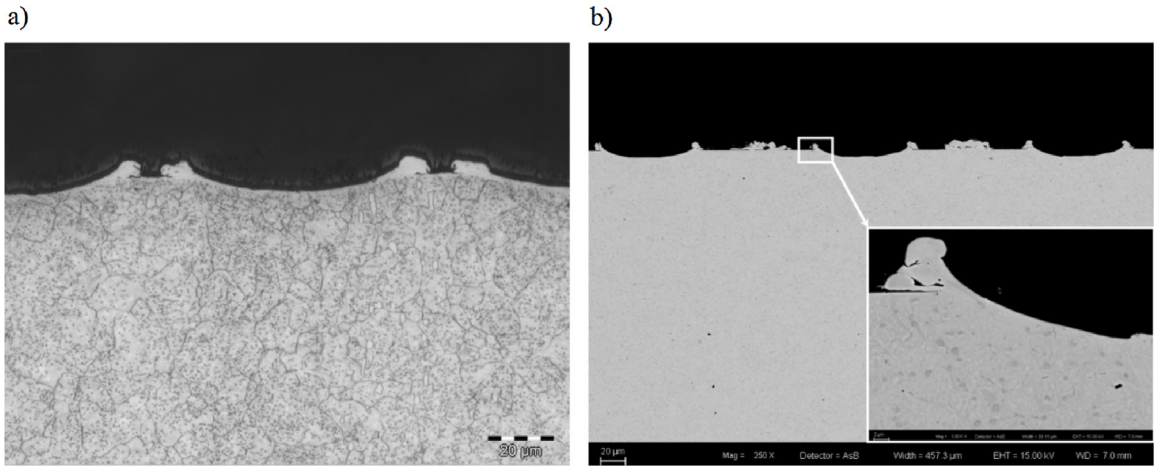

Fig. 3. Cross sections of micro-craters on Uddeholm Rigor polished imprinting dye corresponding to nanosecond pulsed ablation: a) Optical characterization b) SEM characterization. Solid line indicates the heat affected zone after laser ablation.

corresponding yield strength of the substrate. It can be also noted that peak count transfer percentages higher than 100% of the micro-structured imprinting die ($100cm^{-1}$) are obtained for contact pressure values higher than the material yield strength. The results suggest that R_{pc} transfer capability depends on the Rpc value of the strip priori to imprinting process. This is evidenced in the fact that the maximum peak count is found for DP600 which also presented the highest R_{pc} value prior to imprinting tests (Table 2). The two remaining substrates (IF-DX56 and YD220) exhibit similar maximum values as prior to imprinting tests. Thus, the results show peak count to be an extremely sensitive parameter in the imprinting process.

Taking into account the influence of the substrate mechanical properties on the transfer capability of microstructures, an effective contact pressure (ECP) is introduced, defined as the ratio between nominal contact pressure and average yield strength of the substrate. Fig. 6a) shows the roughness transfer capability, fitted to polynomial regression curves, as function of the effective contact pressure (ECP) for the three different material strips. For the ECP range where the roughness transfer capability can be measured for all strip substrates (shadowed area in Fig. 6a) higher transfer capability was observed for materials characterized by higher yield strength values (DP600). This trend is confirmed for R_{pc} transfer where the substrate with higher yield strength point achieve the maximum peak count values at lower ECP.

Based on the suitable roughness parameters (R_a, W_a and R_{pc}), which contribute to improve the appearance of the sheet steel after painting and considering the roughness transfer capability as a function of the material substrate (metal sheets), three selected texture patterns were designed by 3D geometric models (Wentink et al. (2015)). These simulated patterns were selected based on two folds:

- The roughness transfer function of 20% to 60% required an Ra of around 3.5 µm to establish a sheet substrate roughness between 0.7 µm and 2.1 µm in an attempt to also assess the possibility of producing higher roughness values than generally accepted for EDT surfaces. Expected Ra values of the selected patterns range from 3.4 to 3.9 µm.
- The difference between Ra values expected for M1 and M2 motifs are minimal for these designs, which aids stability in the final texturing process and also would allow some mismatch during processing.

Fig. 7 shows the topographical features considered in this research:

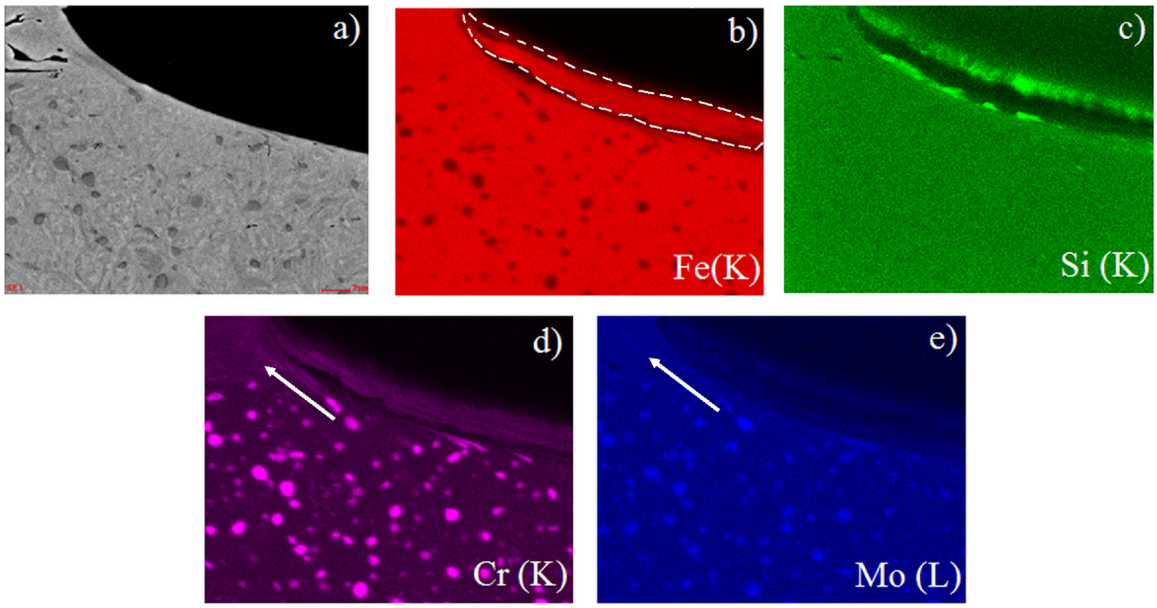

Fig. 4. Elemental mapping of the HAZ and bulk material after laser ablation process for a) un-filtered; b) iron; c) silicon; d) chromium; e) molybdenum content.

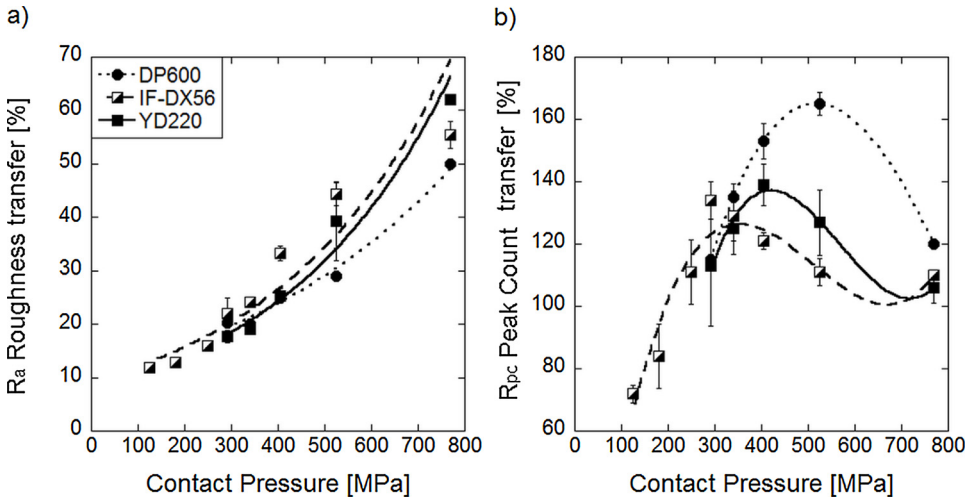

Fig. 5. a) Strip roughness; b) Strip peak count transfer capability as a function of nominal contact pressure for DP600, YD220 and IF-DX56 galvanized substrates imprinted by normal loading with the microsctructured surface described in Fig. 2.

"open" structures, characterized by a different density of hillocks (Figs. 7 a) and b)) and "closed" structures, characterized by a matrix of micro – dimples (Fig. 7 c)). These designed topographical features correspond to the experimental laser texturing configuration described in Fig. 8: two different texturing motifs (rectangular M1 and offset M2) and two crater overlapping degrees (H = V = 90 and H = V = 130), where H and V describe the distances between 2 adjacent craters in the horizontal and vertical directions respectively.

The 3D geometrical model predicts the surface geometry of the imprinting die based on simultaneous texturing events, considering a crater shape characterized by a homogeneous recast layer around the crater rim based on empirical data of single crater morphology. Theoretical roughness determination was achieved by considering overlapping of this recast laser of adjacent craters. In the case of M2H130V130 pattern (Fig. 7c), this overlapping is negligible predicted as in the case of the experimental results of seed pattern (Fig. 2).

4. Results and discussion

4.1. Laser texturing

Fig. 9 gathers the topographies of the three considered textures produced on the imprinting dies. The images combine SEM characterization of the patterns and their surface topography characterization by confocal microscopy on tool steel.

It is worth to note that, in the case of "open" textures (Figs. 9 a) and b)) the random behavior of the material ejected from the inner crater, as well as the overlapping of the remelted material of adjacent craters, promote inhomogeneous structures on the surface topography. In the case of a motif 1 (Fig. 9a), a good match is obtained between the model prediction (Fig. 8a) and the experimental results (Fig. 9a). In the case of motif 2 (Fig. 9b), however, the contribution of the remelted material and crater overlapping is higher and the resulted inhomogeneous rim make it difficult to reproduce experimentally the modelled surface topography set in Fig. 7b). This is not the case of "closed" textures, characterized by a minimum overlapping contribution and, hence, the laser textures match well the optimal design achieved by the geometric model. It is important to point out that the material response to laser pulses depends on the microstructural and optical properties which are not considered in the geometric modelled presented in Fig. 7. Hence, lack of correlation is expected between the laser structures generated experimentally and the modelled ones.

Table 3 shows the topographic and roughness parameters for the three selected textures fabricated by nanosecond pulses. As in the case

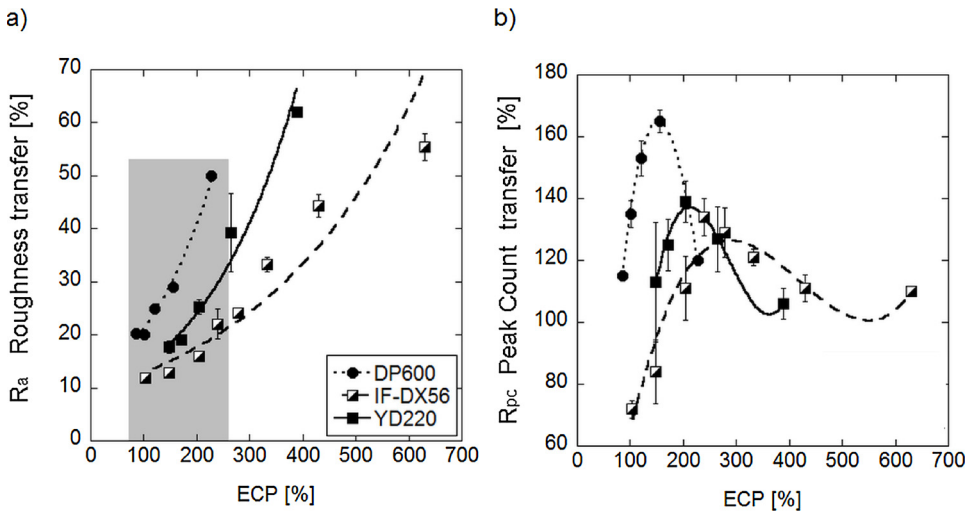

Fig. 6. a) Strip roughness; b) Strip peak count transfer capability as a function of effective contact pressure for DP600, YD220 and IF-DX56 galvanized substrates imprinted by normal loading with the microstructured surface described in Fig. 2.

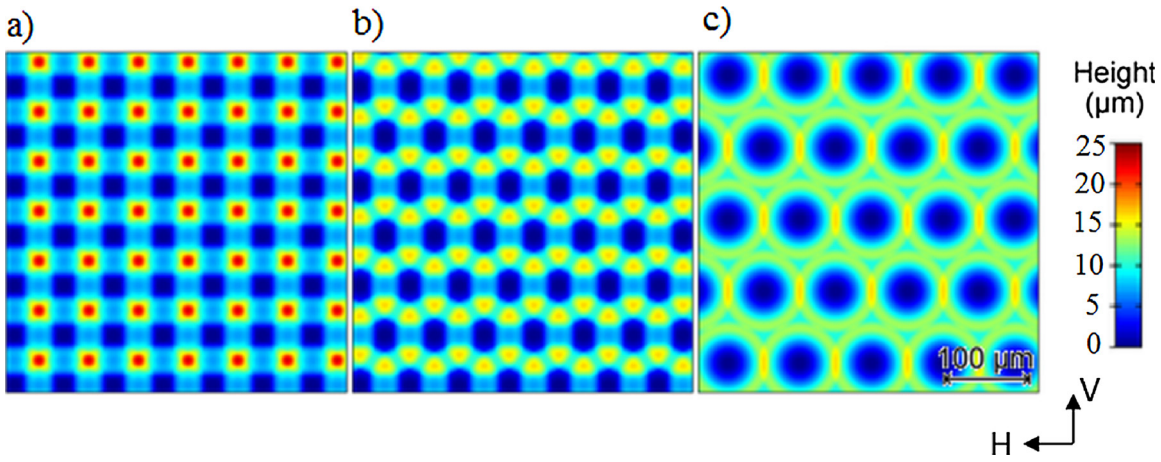

Fig. 7. Top view of the geometric modeling for a) M1H90V90; b) M2H90V90 and c) M2H130V130 patterns.

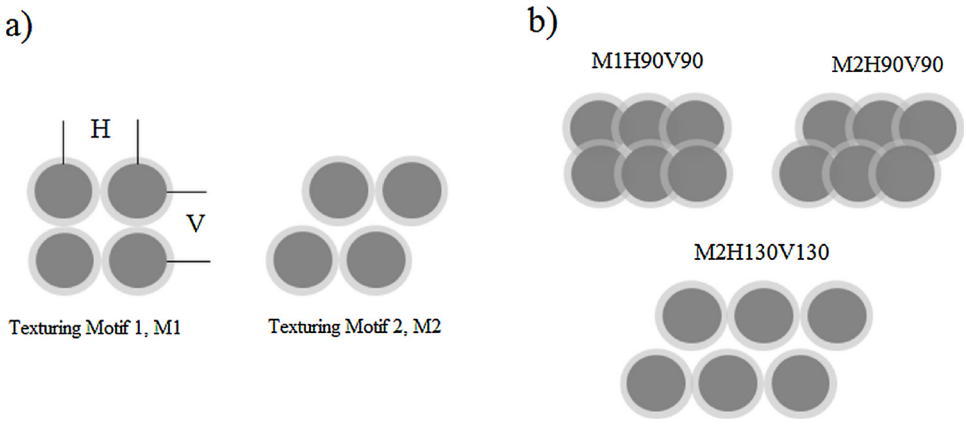

Fig. 8. a) Two different texturing motifs; b) Selected texture patterns.

of isolated craters (Fig. 2b), peak-to-valley height (D) and inner diameter (φ) are gather the topographic information. The peak-to-valley height (D) is introduced only as an estimation as consequence of the random behavior of the ejected material from the inner crater. The roughness values (R_a and R_{pc}) were calculated as average of 5 tracks orientated at 45° with respect to the laser processing direction.

The analysis of the topographic and roughness parameters suggests that:

- Close texture (M_2H130V130) provided the highest values of inner diameter as consequence of non-overlapping pulses strategy as well

Table 3
Topographic and roughness parameters of selected texture patterns on tool steel material.

Pattern	Topographic				Roughness	
	H		V		R_a (μm)	R_{Pc} (cm^{-1})
	D (μm)	φ(μm)	D (μm)	φ(μm)		
M_1H90V90	8	40	5	30	3.1 ± 0.2	158 ± 20
M_2H90V90	8	40	14	50	2.8 ± 0.4	184 ± 26
M_2H130V130	13	65	13	65	3.6 ± 0.2	150 ± 7

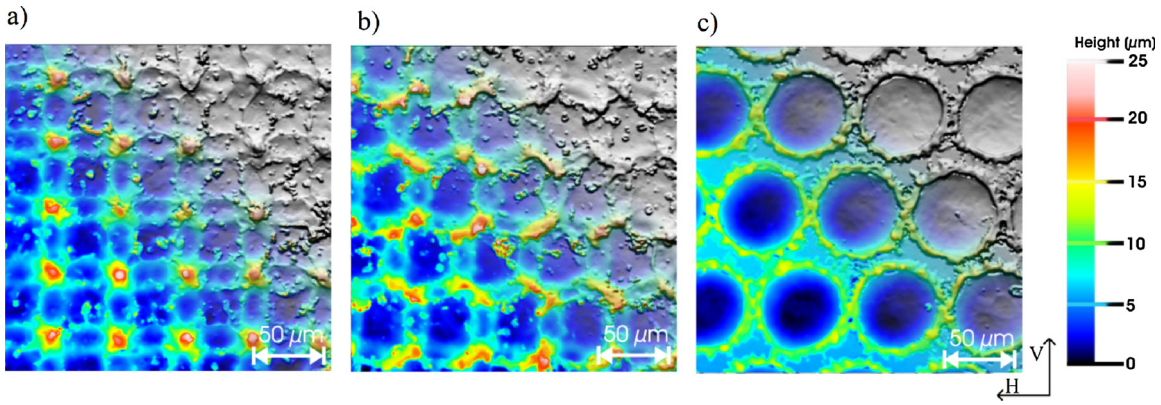

Fig. 9. Grayscale SEM images overlaid with confocal derived height information leading to a joined morphological-topographical characterizations of a) M_1H90V90 b) M_2H90V90 c) M_2H130V130 patterns textured by laser on tool surface. Texturing direction: right-to-left.

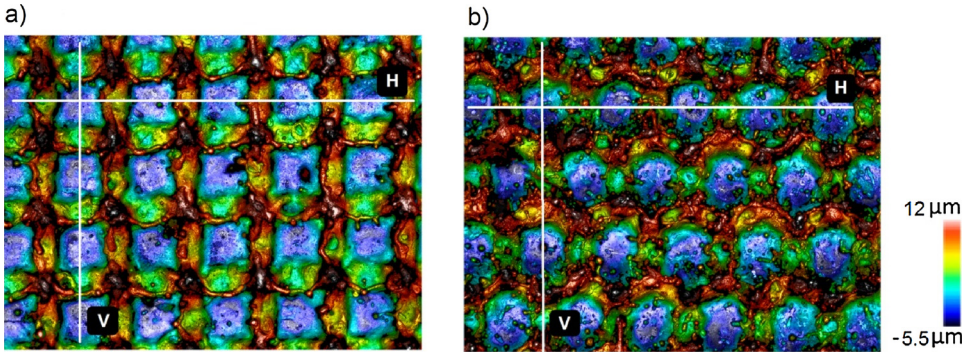

Fig. 10. 3D Confocal image of a) M_1H90V90; b) M_2H90V90 textured patterns.

as a cleat symmetry (between H and V axis) of topographic parameters, which can also be translated as a negligible effect of process direction.

- For a textural design in which overlapping of craters and/or recast material does occur, here denoted by H90V90, different inner diameters along both axes (H and V) could be recognized depending on the considered texturing motif. This can be inspected in more detail in Fig. 10. Significantly different behavior of the ablated material from the inner crater was evidenced between the two motifs. In consequence, a slightly higher inner diameter was found along the V direction in the case of texture motif M_2 (Fig. 10b).
- Textured pattern M2H90V90 provides the highest values of R_{pc}. It could be explained based on the fact that in the case of M2H90V90 less amount of recast material is overlapped compared to M1H90V90 due to the different textured motif considered.

4.2. Normally-loaded roughness transfer tests

The imprinting process was performed on steel grade IF-DX56 considering the three selected textures presented in Table 3. Figs. 11a) c) and e), illustrate the morphological characterization of the textured imprinting die (negative) and Figs. 11 b) d) f) the corresponding ones imprinted strips (positive) for M_1H90V90, M_2H90V90 and M_2H130V130 respectively. It is noteworthy that a homogeneous pattern transfer is obtained in both directions for the three textured patterns. Figs. 11b) and d) disclose the transfer of the dimple center and the overlapped area between consecutive dimples. Additionally, in the case of M_2H90V90 a random contribution of features < 10 µm in diameter is evidenced, in the positive (Fig. 11d)) and negative (Fig. 11c)) patterns, as consequence of the overlapping of the recast material. For M_2H130V130 the non-overlapped recast material of the negative pattern (Fig. 11e)) is transferred to the positive (Fig. 11f)) one as a regular groove around the dimple. Moreover, the unprocessed material between the dimples is observed in both the positive and negative patterns.

Figs. 12a) and b) disclose the roughness and peak count transfer respectively as function of effective contact pressure. For the considered textures, roughness transfer functions (Fig. 12a) present an almost linear increase when increasing the effective contact pressure, reaching maximum transfer percentages (in the case of M2H90V90) of almost 50% at 1.25 times the yield strength for the considered substrate (Table 2). The R_a values of the strips are in the target range (0.7 µm < R_a < 1.5 µm) typically requested by the automobile industry. It is important to point out that the lowest roughness transfer values are found in the case of M2H130V130, corresponding to the highest Ra values on the imprinting die (Table 3). The results of Ra transfer capability also suggest that, for the considered range of EPC, there seems to be a maximum value of Ra to be achieved on the imprinting strips (at around 1.4 µm) regardless of Ra imprinting die. Both the linear trend and the roughness transfer values observed for the three textures are in agreement with the results achieved for the seed pattern in the case of IF-DX56 substrate (Fig. 6a) for the considered pressures range. Considering the R_{pc} values of the textures of imprinting dies (Table 3), the imprinted strips achieve $R_{pc} > 75cm^{-1}$ for the three textures and the contact pressure range considered. Two remarkable trends are recognized for open (M1H90V90 and M2H90V90) and close (M1H130V130) textures. It is evidenced a remarkable increase of transfer percentage (up to 130%) in the case of close texture compared to the maximum values obtained for open textures (94%) for contact pressures higher than 3 times the substrate yield strength. The latter finding could be associated to the different R_{pc} roughness transfer function when open or closed patterns are considered. Based on previous studies from the authors (Wentink et al., 2015),Chichkov et al., 1996 it could be explained by the differences in bearing area between imprinting die and strip when open and close textures are considered. On the other hand, the peak count transfer of closed-type textures ratifies the performance evidenced in the case of the seed texture (Fig. 6b) and the transfer percentages in the effective contact pressure ranges considered are the same in both cases for IF-DX56 substrate. That is to say, in both cases, for the IF-DX56 substrate, a maximum peak count transfer was achieved at about EPC between 250 and 350% followed by a drop-off. In the case of open textures the peak count transfer function reveals a more stable upper limit.

4.3. Paint appearance

Fig. 13 a) reveals the waviness results for the surfaces described above whose roughness meets the requirements regarding roughness (around R_a = 1.3 µm, 0.8 mm filter and $R_{pc} > 75cm^{-1}$) along with a reference corresponding to a EDT surface where the same roughness was induced, prior to painting. The results show that the surfaces whose finish is attained by laser texturing show a remarkable decrease of the waviness values (over all common length scales W_a(0.8–2.5), $W_{a(2.5–8)}$ and $W_{a(1}$–5)) considering $R_{pc} > 75cm^{-1}$ and 0.7 µm < R_a < 1.5 µm. Samples of galvanised IF-DX56 produced under compression tests were painted with the e-coat layers using the modular paint line described in section 2. Fig. 13 b) reveals the LW and SW results as recorded using a BYK Gardener Wavescan, after application of Nitto tape – an industry standard for simulating paint clear coat layers. Both results emphasise the significant improvement related to EDT surfaces as consequence of the process window enlargement enabled by laser texturing and may enable a possibility to reduce paint layer thicknesses in the future and thus its environmental impact, while maintaining acceptable paint appearance for consumers.

Fig. 14 summarizes the final main roughness parameters in IF-DX56 galvanised steel strips obtained after imprinting process for the three designed textures before painting process. The results exhibit that new surfaces produced by laser technology, for the entire pressure range between 250 MPa and 500 MPa, fulfil the requirements for improving paint appearance: Rpc > 75 cm^{-1}, 0.7 µm < R_a < 1.5 µm and

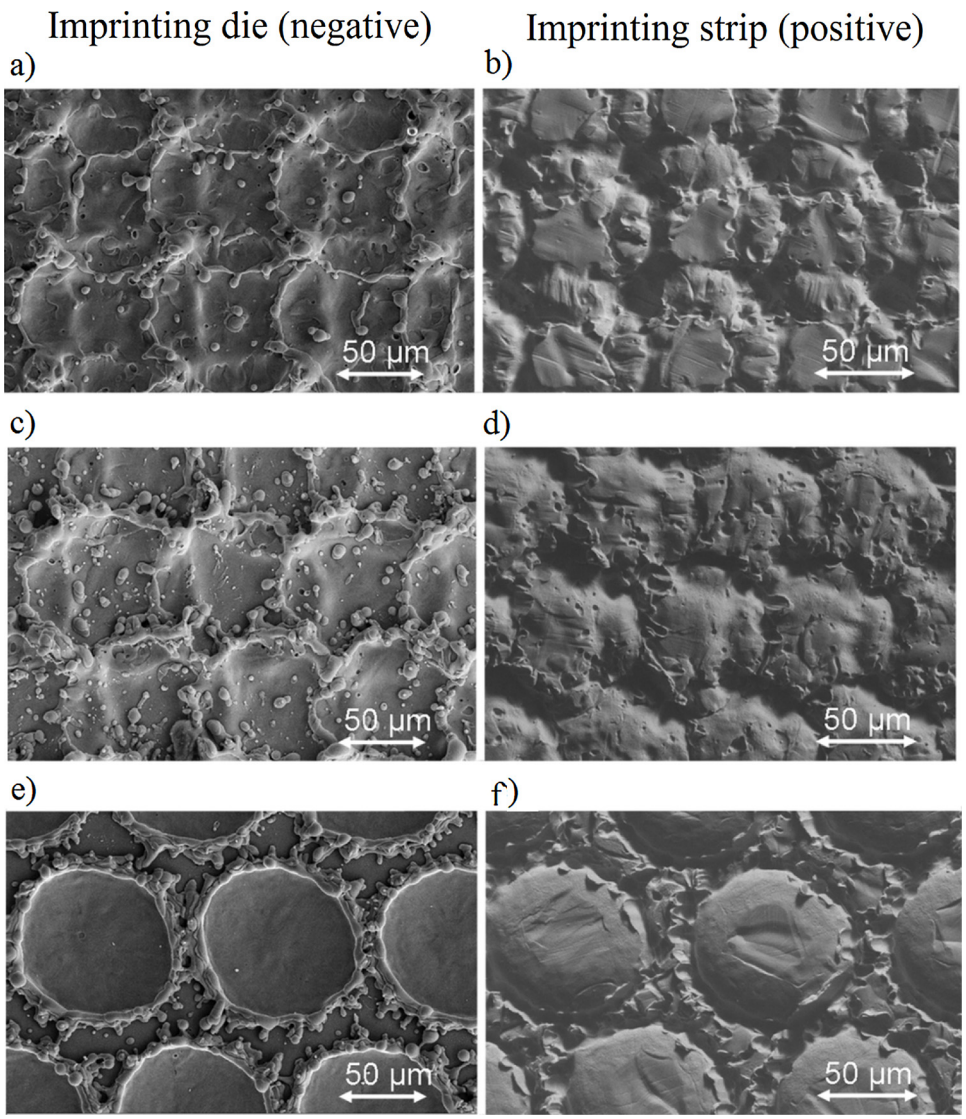

Fig. 11. SEM images of textured imprinting die (negative) and imprinting strip (positive) of a) b) M1H90V90; c)d) M2H90V90 and e)f) M1H130V130 surface textures.

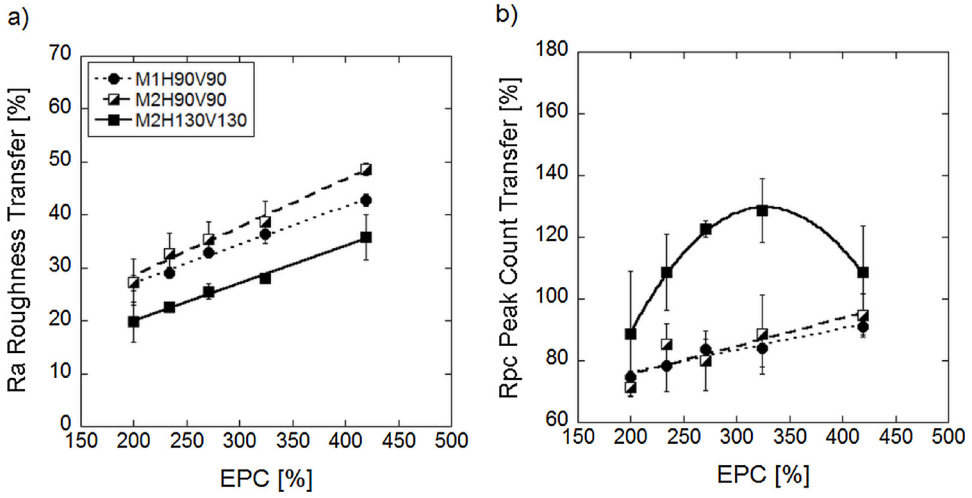

Fig. 12. a) Strip roughness; b) Strip peak count transfer capability as a function of absolute nominal pressure for IF-DX56 galvanized substrates imprinted by normal loading with the textured surface described in Fig. 11.

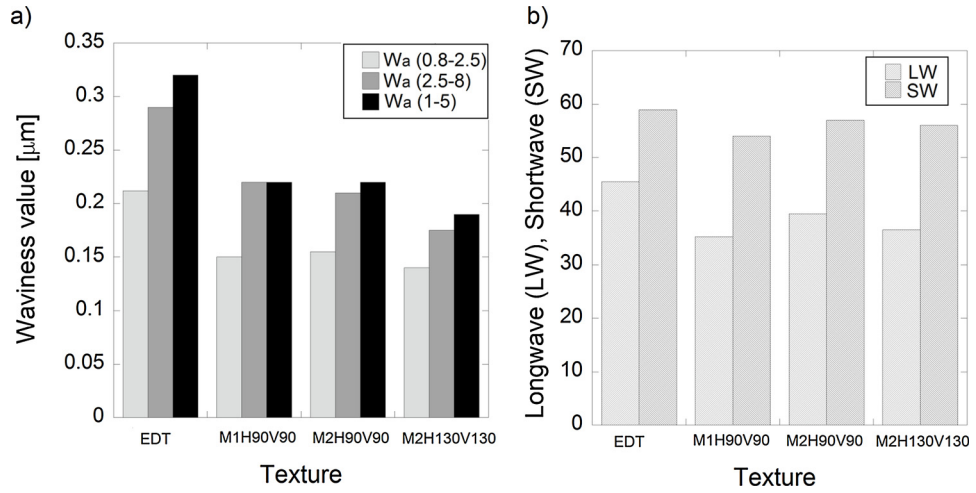

Fig. 13. a) Surface waviness; b) LW and SW values for e-coat surfaces of three surfaces generated by imprinting of laser-textures tools in IF-DX56 galvanised steel and a EDT reference. All surfaces had an Ra of.1.3 μm–1.4 μm.

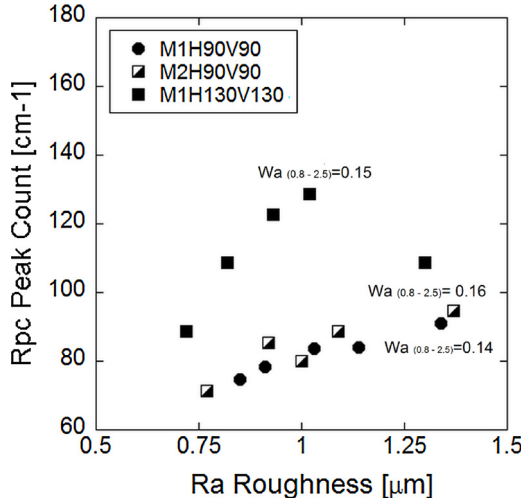

Fig. 14. Roughness (Ra), Peak count (Rpc) and Waviness (Wa) for the three surfaces generated by imprinting of laser-textures tools in IF-DX56 galvanised steel.

$0.1\,\mu m < W_a < 0.4\,\mu m$. Compared to textures obtained by EDT a decrease of waviness values along with an increase of R_{pc} are obtained.

5. Conclusions

This study assesses laser surface texturing as an innovative technology to control and improve appearance after painting of metal strips obtained during the roll imprinting process based on theoretical surface design. It involved using a short-pulsed laser texturing process on tool steel samples to generate a series of negatives of the final textures derived based on a geometric model to be achieved on the metal strips considering the roughness transfer during the compression tests, which replicate the skin-pass rolling. The following conclusions can be drawn from the experimental results:

- For an initial seed pattern (closed dimples) the transfer capability of R_a follows a exponential growth as function of the effective contact pressure for the three considered substrates reaching maximum transfer percentages of 60%. In the case of R_{pc}, the roughness transfer results disclose a maximum value at contact pressures corresponding to the substrate yield strength that tens to the peak count of the textured tool steel (negative) when the normal load increases above the yield strength point. For both transfer functions, a significant dependence with the substrate was thus disclosed.
- Three negative textures (two open and one closed dimples) were designed to meet the current requirements of roughness, peak count and waviness on the final steel strips (positive textures) for the automotive industry. The morphological characterization of the positive textures (IF-DX56) after compression tests reveals a homogeneous transfer of the negative patterns.
- The roughness transfer on IF-DX56 for the three final textures follows the same trend as in the case of the seed pattern. The peak count (spatial) transfer function exhibits different behavior for open and closed dimples.
- Comprehensive surface characterizations of the laser textured samples in terms of topography, morphology and microstructural changes induced by the laser radiation were performed.
- e-coat layers were applied on the positive textures created on IF-DX56 by compression tests. Waviness results reveals a significant decrease of waviness values overall length scales considering $R_{pc} > 75 cm^{-1}$ and $0.7\,\mu m < R_a < 1.5\,\mu m$, which represents an important enlargement of the process window to produce next-generation outer panels for the automotive industry and a possibility to reduce the environmental impact of paint use through reduced paint layer thicknesses in the future.
- A new procedure to produce new textures on galvanized steel by laser texturing was developed. The novel surfaces exhibit, for the required R_a range, a decrease of waviness values along with an increase of R_{pc} resulting in superior paint appearance with respect to the textured generated by EDT surfaces.

Further investigations about the transfer capability behavior of a wider range of deterministic patterns produced by pulsed laser texturing technique area being explored as well as the possibility to perform the laser texturing process under different environmental conditions to improve surface mechanical properties with the aim to reduce roll wear during skin pass rolling.

Acknowledgements

The authors gratefully acknowledge the work of Jan Wormann and Willem van Leeuwen (Tata Steel R&D). The research leading to these results has received funding from the European Community's Research Fund for Coal and Steel (RFCS) under grant agreement n° [RFSR-CT-2011-00022], STEELTAC project.

References

Bastawros, A., Speer, J.G., Zerafa, G., Krupitzer, R., 1993. Effects of steel surface texture on appearance after painting. SAE Technical Paper Series, 930032.

Chichkov, B.N., Momma, C., Nolte, S., von Alvensleben, F., Tünnermann, A., 1996. Femtosecond, picosecond and nanosecond laser ablation of solids. Applied Physics A 63 (2), 109–115. https://doi.org/10.1007/BF01567637.

Costil, S., Lamraoui, A., Langlade, C., Heintz, O., Oltra, R., 2014. Surface Modifications induced by pulsed-laser texturing – influence of laser impact on the surface properties. Appl. Surf. Sci. 288, 542–549.

De Mello, J.D.B., Gonçalves Jr., J.L., Costa, H.L., 2013. Influence of Surface texturing and hard chromium coating on the wear of steels used in cold rolling mill rolls. Wear 302 (1–2), 1295–1309.

Demir, A.G., Maressa, P., Previtali, B., 2013. Fibre laser texturing for surface functionalization. Phys. Proc. 41, 759–768.

Du, D., He, Y.F., Sui, B., Xiong, L.J., Zhang, H., 2005. Laser texturing of rollers by pulsed Nd:YAG laser. J. Mater. Process. Technol. 161, 456–461.

Elkoca, O., 2008. A study on the characteristics of electrical discharge textures skin pass mill work roll. Surf. Coat. Technol. 202 (12), 2765–2774.

EN 10049, 2014. Measurement of Roughness Average Ra and Peak Count RPc on Metallic Flat Products.

Hilgenberg, K., Steinhoff, K., 2015. Texturing of skin-pass rolls by pulsed laser dispersing. J. Mater. Process. Technol. 225, 84–92.

Jaggessar, A., Hesam, S., Mathew, A., Yarlagadda, P.K.D.V., 2017. Bio-mimicking nano and micro-structured surface fabrication for antibaterial properties in medical implants. J. Nanobiotechnology 15, 64.

Kijima, H., 2014. Influence of roll radius on roughness transfer in skin-pass rolling of steel strip. J. Mater. Process. Technol. 214, 1111–1119.

Kijima, H., 2015a. Influence of lubrication on roughness crushing in skin-pass rolling of steel strip. J. Mater. Process. Technol. 216, 1–9.

Kijima, H., 2015b. An experimental investigation on the influence of lubrication on roughness transfer in skin-pass rolling of steel strip. J. Mater. Process. Technol. 225, 1–8.

Kimura, Y., Ueno, M., Mihara, Y., 2009. Printing behavior of roll surface texture to hot-dip galvanized steel sheet in temper rolling. TetsutoHagan 95 (5), 399–405.

Mezghani, S., Zahouani, H., Piezanowski, J.-J., 2011. Multiscale characterizations of painted surface appearance by continuous wavelet transform. J. Mater. Process. Technol. 211, 205–211.

Quintana, I., Rodríguez, E., Viteri, V.Sde., Matthews, D., Wentink, D.J., Elliot, L.C., Korver, F., 2014. Texturing of imprinting dies using nanosecond pulses. Applications for automotive industry. KES Transactions on Sustainable Design and Manufacturing 1 (1) Special Edition - Sustainable Design and Manufacturing.

Scheers, J., De Maré, C., Meseure, K., 1996. SIBETEX: steel's contribution to an improved paint appearance for outer car body panels. Proceedings IBEC'96. pp. 24.

Scheers, J., Vermeulen, M., De Maré, C., Meseure, K., 1998. Assessment of steel surface roughness and waviness in relation with paint appearance. International Journal of Machine Tools and Manufacture 38 (5–6), 647–656. https://doi.org/10.1016/S0890-6955(97)00113-2.

SEP 1941, 2012. Measurement of the Waviness Characteristic Value Wsa(1-5) on Cold Rolled Metallic Flat Products.

Vermeulen, M., Scheers, J., 2001. Micro-hydrodynamic effect in EBT textured steel sheet. Int. J. Mach. Tools Manuf. 41 (13–14), 1941–1951.

Wan, D., Liu, H., Wang, Y., Hu, D., Gui, Z., 2008. CO_2 laser beam modulating for surface texturing machining. Opt. Laser Technol. 40, 309–314.

Wentink, D.J., Matthews, D., Appelman, N.M., Toose, E.M., 2015. A generic model surface texture development, wear and roughness transfer in skin pass rolling. Wear 328–329, 167–176.